論文 / 著書情報
Article / Book Information

Title	Optical quantification of suffosion in plane strain physical models
Authors	Mao Ouyang, Akihiro Takahashi
Citation	Géotechnique Letters, Vol. 5, Issue 3, pp. 118-122
Pub. date	2015, 9
DOI	http://dx.doi.org/10.1680/jgele.15.00038
Note	This file is author (final) version.

Title:

Optical quantification of suffosion in plane strain physical models

Authors:

Mao Ouyang

PhD candidate, Department of Civil Engineering, Tokyo Institute of Technology, Tokyo, Japan

Akihiro Takahashi

Professor, Department of Civil Engineering, Tokyo Institute of Technology, Tokyo, Japan

Corresponding author:

Name: Akihiro Takahashi

Contact address: 2-12-1-M1-3 Oh-okayama, Meguro, Tokyo 152-8552, Japan

Telephone: +81-(0)3-5734-2593

E-mail: takihiro@cv.titech.ac.jp

Géotechnique Letters 5 (3), 118-122, 2015.
Original URL:
http://dx.doi.org/10.1680/jgele.15.00038

Abstract:

Suffosion is a seepage-induced instability phenomenon whereby fines are eroded away through the constrictions formed by coarse particles, resulting in a reduction in soil volume and a change in hydraulic conductivity. In this study, upward seepage tests were performed on gap-graded soil containing coloured fines in a plane strain apparatus. A series of images was recorded through a transparent window to quantify the features of suffosion. The estimated cumulative eroded soil mass from image analysis was found to generally agree with independent macroscopic observations, indicating that optical analysis allows an easy identification of suffosion characteristics. For the tested soil, the fines were prone to be transported within an instant period of increasing hydraulic gradient, with few of them moving during the constant flow. Furthermore, the volume of the specimen was reduced due to suffosion, leading to an alternation of preferred coarse particle orientations in the observation field.

KEYWRODS: erosion; microscopy; fabric/structure of soils; seepage

NOTATION

f_c	fines content
e_{max}	Maximum void ratio
e_{min}	Minimum void ratio
d_{50}	Median particle size
C_c	Curvature coefficient
C_u	Uniformity coefficient
ε_v	Volumetric strain
e_0	Initial void ratio
Δ	Vector magnitude
N	Total number of particles
$\mathbf{n}$	Unit vector
φ_k	Inclination of unit vector

INTRODUCTION

It is known that the microstructure of soil can be changed by suffosion, which is an instability phenomenon whereby fines are eroded away from the specimen due to seepage flow, yielding a reduction in total volume and a change in hydraulic gradient. Rosenbrand & Dijksra (2012) quantitatively investigated the spatial distribution of fines by image analysis. Correia dos Santos et al. (2015) visually observed the transportation of fines in gap-graded soils, which threw light on the design of embankment core materials.

The image processing technique was also applied in this research to quantitatively describe the characteristics of suffosional soil based on images recorded by a digital microscope (Hirox VCR-800). This device is equipped with a compact 2·11 million pixel charge coupled device (CCD) camera that is capable of capturing high-quality colour images consisting of 1600 and 1200 effective pixels in the horizontal and vertical axis respectively.

In this study, images were analysed using the open-source computer vision library (opencv) (Bradski, 2000), by which digital images can be viewed as two-dimensional discrete components of spatial coordinates and the magnitude of feature value of three colour components (R (red), G (green) and B (blue)). Calibration of the microscope indicated that there was only 1·33% area distortion and therefore the influence of lens distortion was neglected in the image processing. According to the distinct colours of fines and coarse particles, their spectra could be recognised from the original recorded image and then segmented in order to calculate the fines content. Figures 1(a) and 1(b) show a typical original image and a segmented image respectively. The movement of fines at the onset of suffosion was quantitatively obtained by comparing the locations of fines on two successive images, which is termed image subtraction. To detect the contours of coarse particles, the watershed algorithm was utilised. The change of preferred coarse particle orientation was identified from the outlines of individual coarse particles in the images taken before and after suffosion, as illustrated in Fig. 1(c). Figure 1(d) illustrates the preferred coarse particle orientation and aspect ratio, which will be discussed later.

This paper briefly describes the one-dimensional upward seepage tests performed on gap-graded soils containing different initial fines contents. By analysing the images recorded during the seepage tests, the characteristics of suffosion were quantitatively assessed with respect to cumulative eroded soil mass, fines transportation at the onset of suffosion and volume reduction accompanied with the alternation of preferred coarse particle orientation.

EXPERIMENTAL SETUP

The test material in this study was a mixture of silica no. 3 and silica no. 8. The natural grey silica no. 3 was regarded as the coarse particles, which forms the soil skeleton. The silica no. 8 was artificially coated with blue pigment and then stabilised by baking; this was treated as fines, which could be eroded away by seepage flow. All specimens, with initial fines contents of 15%, 25% and 35%, were prepared by the moist tamping method targeting 30% relative density to ensure the occurrence of suffosion, with an initial water content of around 5%. The properties of the siliceous sands and mixtures are summarised in Table 1 and the corresponding particle size distributions are shown by the solid lines in Fig. 2.

Upward seepage tests were performed on the gap-graded specimens. Figure 3 shows a schematic diagram of the test apparatus, which mainly comprised a rectangular seepage cell with a transparent window in the front and a water tank. The specimens were 100 mm wide, 35 mm deep and 60 mm high. Inlet flow was provided from the water tank, which could be raised or lowered to control the head difference assigned on the specimen. A 30 mm thick gravel diffusing filter was placed in the bottom of the specimen box to ensure a reasonably uniform flow across the soil and non-woven textile was placed below the specimen to prevent downward fines loss. A cylinder was installed at the outlet to measure the average flow velocity.

After completion of specimen preparation, water was allowed to continuously and gently flow through the soil until it became saturated. A series of images was recorded at different locations through the transparent window to analyse the soil structure after saturation. The microscope was then fixed on the middle of the specimen through the front transparent window in order to observe the micro- structural evolution of the soil subjected to suffosion. The water tank was raised to increase the water head on the bottom of the specimen. For each increment, a time of 30 min was allowed to ensure completion of particle transportation. The increase in water head was repeated until no movements could be observed. The microscope was then moved to record images at various locations on the front transparent window, which were to be interpreted to acquire an understanding of the particle spatial distribution of suffosional soil.

TEST RESULTS AND DISCUSSIONS

Cumulative eroded soil mass

A summary of the test results, including the maximum as- signed hydraulic gradient, cumulative eroded soil mass and volumetric strain at the end of the test, is given in Table 2. After termination of the seepage test, the soil was collected and dried to obtain its particle size distribution. The particle size distributions of the soil after suffosion are plotted as dashed lines in Fig. 2. The figure shows that the particle size distribution shifted downwards after the experiment, suggesting fines loss due to suffosion. The percentages of cumulative eroded soil mass were calculated by employing the method proposed by Kenney & Lau (1985) who derived the percentage of fines loss by the amount of shift of the distribution curve. The results are shown in Fig. 4.

Based on colour distinction, image segmentation was applied to the images of the suffosional soils to obtain the spatial distributions of both fines and coarse particles. Repeatable and representative results of the derived cumulative eroded soil mass depend on the number of images applied in the analysis; therefore, 27 images taken from various locations on the transparent window were utilised. The deviation of cumulative eroded soil mass from the independent macroscopic observations against the number of images is shown in Fig. 5. The figure shows that one image (of size 8 mm × 6 mm) is not sufficient to obtain a reasonable value, but 20 images, representing around 960 mm2 (15% of the total front area), yields a reasonable result.

The cumulative eroded soil masses estimated using image segmentation are plotted in Fig. 4, and there is good agreement between these values and the data from independent macroscopic observations. An average deviation of approximately 5% suggests that the image analysis technique is capable of describing suffosion properties.

Fines transportation at onset of suffosion

The hydraulic gradient at the onset of suffosion was defined as the initiation hydraulic gradient by Chang & Zhang (2013). That is, under the initiation hydraulic gradient, fines start to move (Skempton & Brogan, 1994). The relationship between hydraulic gradient and average flow velocity of the specimen with 15% initial fines content at the initial stage of suffosion is shown in Fig. 6. It can be seen that the hydraulic conductivity started to change when the hydraulic gradient reached 0·22; this was regarded as the initiation hydraulic gradient in this test case. Five successive images over 30 s covering the period of the onset of suffosion were then analysed to assess fines transportation in microscale.

Figure 7 demonstrates the mobile portions, consisting of the appearance and disappearance of fines, together with the hydraulic gradient. The mobile portion is defined as the fraction of area where fines move relative to the total image area with the underlying assumption that the disappearance of fines from the consequential image means they are transported by seepage flow. Figure 7 shows that the major movements occurred during an increase in hydraulic gradient, with little transportation of fines during constant flow. Similar phenomena were observed in the different increment steps during the seepage tests. It could be argued that the movement of fines observed through the transparent window might be different from that in the inside of the specimen and that the stress states in the physical model could be different from that in situ, and these points might be considered an inherent limitation of this analysis. However, the consistency of the above description with others in the literature (Moffat et al., 2011; Rosenbrand & Dijksra, 2012; Horikoshi & Takahashi, 2014; Ke & Takahashi, 2014) may well demonstrate the applicability of the current method to detect the onset of suffosion.

Preferred coarse particles orientation

As indicated in Table 2, specimen volumes were reduced due to suffosion, which might be due to loss of fines and the rearrangement of particles. Two images taken at hydraulic gradients of approximately 0·65 and 0·70 for the specimen with 15% initial fines content show the movements of a coarse particle at the microlevel (Fig. 8). It can be seen that not only translation, but also rotation, of coarse particles occurred within the period of increasing hydraulic gradient.

To quantify the influence of suffosion on the soil, the watershed algorithm was applied to obtain the outline of coarse particles and then to calculate the preferred particle orientation. The vector magnitude Δ proposed by Curray (1956) was employed to characterise the intensity of the preferred coarse particle orientation, expressed as

$$\Delta = \frac{1}{2N}\sqrt{\left(\sum_{k=1}^{2N}\cos 2\varphi_k\right)^2 + \left(\sum_{k=1}^{2N}\sin 2\varphi_k\right)^2} \qquad 1$$

where N is the total number of particles and φ_k is the inclination of the kth unit vector **n** (see Fig. 1(d)), which varies from zero for an isotropic particle arrangement to unity when all particle orientations are exactly the same. In the upward seepage test, it is expected that a change in the metastable structure might be trigged by the water flow, resulting in a horizontal distribution of preferred coarse particle orientation due to gravity acting on the particles.

Through image analysis, 200 coarse particles randomly selected from images taken before and after the seepage test for the specimen with 15% initial fines content were numbered and their orientations identified. The orientations with respect to the horizontal are shown in a rose diagram representation in Fig. 9. The value of Δ of the specimen before suffosion was 0·091, which suggests that the specimen prepared by the moist tamping method tended to be isotropic (Yang et al., 2008), as expected. Regarding the soil after suffosion, no particular preferred orientation was detected, and the Δ value was 0·052. However, since coarse particles could be categorised as subangular particles (with an average aspect ratio of 0·80 (Fig. 1(d)) (Altuhafi et al., 2013), the reduction of Δ by 42·9% might suggest that the force transformation along the coarse particles could be alternated due to suffosion. Moreover, Fig. 9 indicates that many of the coarse particles were arranged horizontally after suffosion.

CONCLUSIONS

In this study, image analysis was applied to quantitatively describe the characteristics of soil subjected to suffosion. The cumulative eroded soil masses calculated by means of image analysis were generally in accordance with those obtained from independent macroscopic observations, suggesting that image analysis is an effective tool for describing the features of suffosion. For the gap-graded soil studied in this research, during an increase in hydraulic gradient, a large amount of fines tended to be transported, but were prone to be stationary under constant flow. The volume of the soil specimens decreased due to suffosion and, as a result, the coarse particles were oriented horizontally.

ACKOWNLEDGMENT

Support for the first author is provided by a Monbukagakusho (Ministry of Education, Culture, Sports, Science and Technology, Japan) scholarship for graduate students. This work was supported by JSPS KAKENHI grant number 25420498.

REFERENCES

Altuhafi, F., O'Sullivan, C. and Cavarretta, I. (2013). Analysis of an image-based method to quantify the size and shape of sand particles. *J. Geotech. Geoenviron. Eng.* **139**, No. 8, 1290-1307.

Bradski, G. (2000). The opencv library. *Doctor Dobbs Journal.* **25**, No. 11, 120-126.

Chang, D.S. & Zhang, L.M. (2013). Critical hydraulic gradients of internal erosion under complex stress state. J. Geotech. Geoenviron. Eng. 130, No. 9, 1454-1467.

Correia dos Santos, R.N., Caldeira, L.M.M.S. & Maranha das Neves, E. (2015). Experimental study on crack filling by upstream fills in dams Géotechnique 65, No. 3, 218-230.

Curray, J.R. (1956). The analysis of two-dimensional orientation data. J. Geol. 64, No. 2, 117-131.

Horikoshi, K. & Takahashi, A. (2014). Physical model tests on suffosion-induced change of spatial distribution of fine fraction in embankment. In *Proceedings of the 7th International Conference of Scour and Erosion* (Cheng, L., Draper, S. & An, H. (eds)). London: Taylor & Francis, pp.163-170.

Ke, L. & Takahashi, A. (2014). Experimental investigations on suffusion characteristics and its mechanical consequences on saturated coheshionless soil. *Soils and Found.* **54**, No. 4, 713-730.

Kenney, T.C. & Lau, D. (1985). Internal stability of granular filters. *Can. Geotech. J.* **22**, No. 2, 215-225.

Moffat, R., Fannin, R.J. & Garner, S.J. (2011). Spatial and temporal progression of internal erosion in cohesionless soil. *Can. Geotech. J.* **48**, No. 3, 399-412.

Rosenbrand, E & Dijksra, J. (2012). Application of image subtraction data to quantify suffosion. *Géotechnique Letters* **2**, No. 2, 37-41.

Skempton, A.W. & Brogan, J.M. (1994). Experiments on piping in sandy gravels. *Géotechnique* **44**, No. 4, 449-460.

Yang, Z.X., Li, X.S. & Yang, J. (2008). Quantifying and modelling fabric anisotropy of granular soils. *Géotechnique* **58**, No. 4, 237-248.

Table 1. Properties of tested materials

Specimen	Silica No. 3	15% initial fines content	25% initial fines content	35% initial fines content	Silica No.8
Fines content, *fc*: %	0.0	15.0	25.0	35.0	100.0
Maximum void ratio, e_{max}	0.94	0.79	0.77	0.74	1.33
Minimum void ratio, e_{min}	0.65	0.53	0.37	0.36	0.70
Median particle size, d_{50}: mm	1.76	1.78	1.69	1.54	0.16
Curvature coefficient, C_c	0.96	8.69	8.54	0.07	0.99
Uniformity coefficient, C_u	1.31	13.0	16.4	19.3	1.05

Table 2. Summary of test results

Test case	Initial fines content: %	Initial void ratio, e_0	Maximum assigned hydraulic gradient	Cumulative eroded soil mass: g	Volumetric strain, ε_v: %
1	15	0.71	1.1	34.54	2.5
2	25	0.65	1.2	44.34	4.2
3	35	0.63	1.0	61.45	5.8

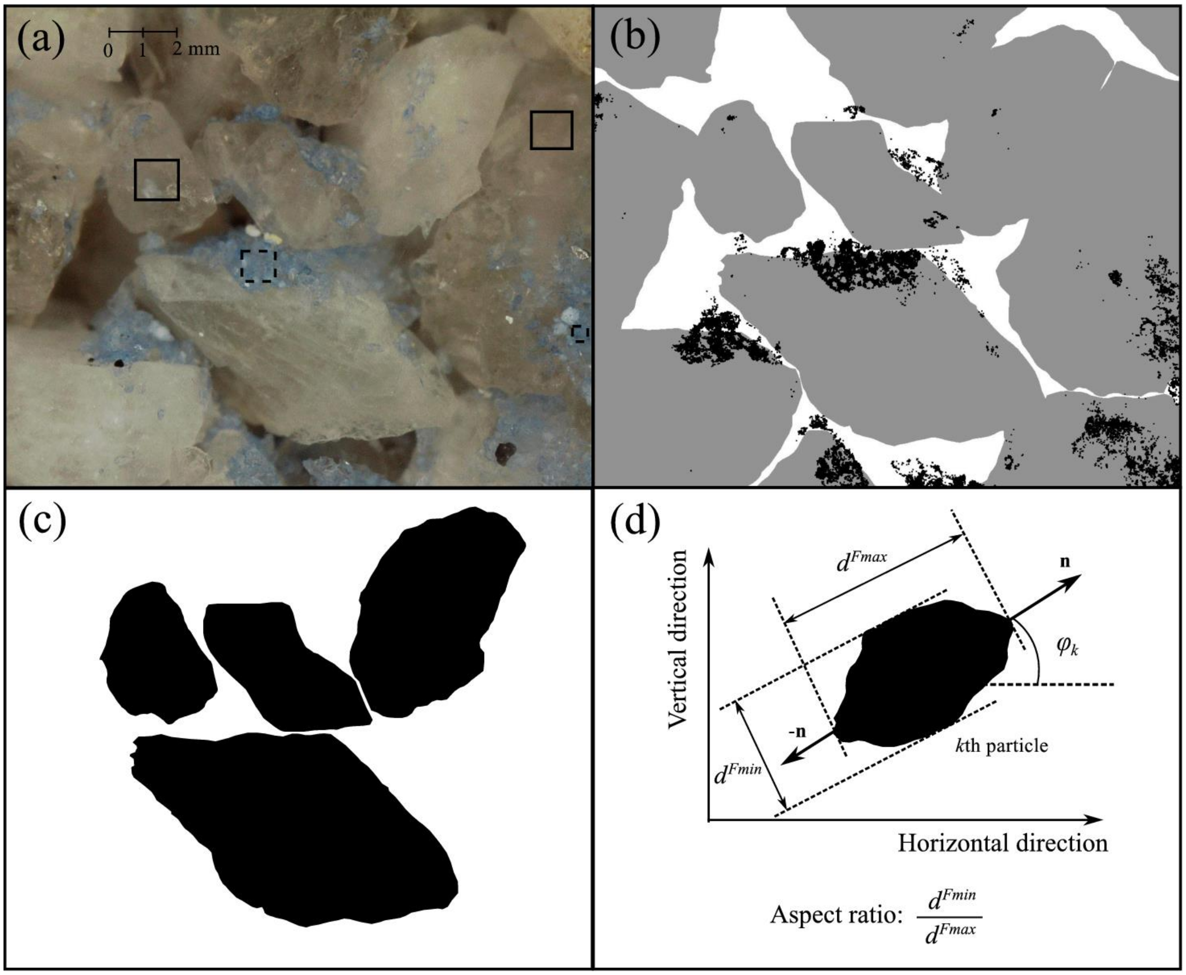

Fig. 1. (a) Original image taken by microscope VCR-800; the spectrum of fines is obtained from the dash blocks, and the spectrum of coarse particles is obtained from the solid blocks. According to the spectrum distinction between the fines and coarse particles, they can be segmented from the original image and is shown in (b) segmented image, where the black areas represent the fines; and the grey areas represent the coarse particles; (c) outline of the coarse particles by watershed algorithm; (d) illustration of preferred coarse particles orientation, and aspect ratio which is the ratio of the minimum distance to the maximum distance between two parallel tangential lines restricting the particle

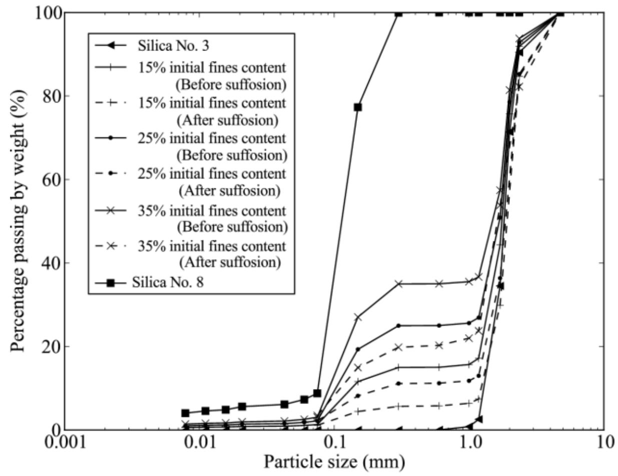

Fig. 2. Particle size distributions

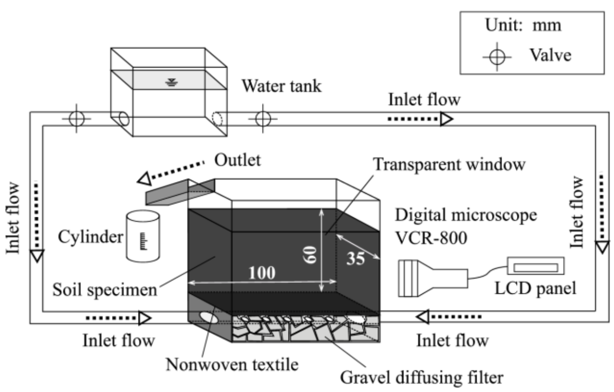

Fig. 3. Schematic diagram of seepage test apparatus

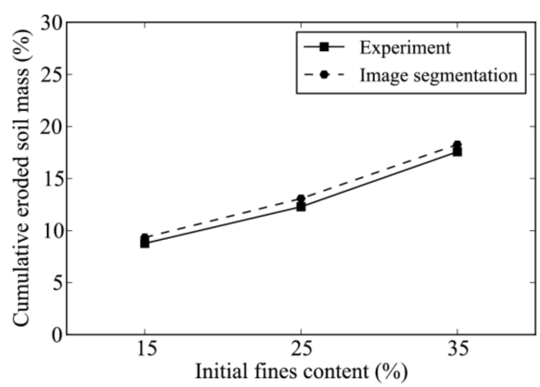

Fig. 4. Cumulative eroded soil mass obtained from experiment and image segmentation

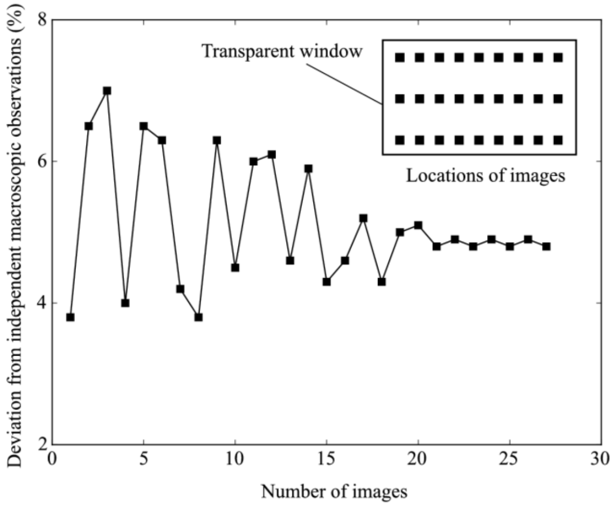

Fig. 5. Deviation from the independent macroscopic observations against number of images (15% initial fines content)

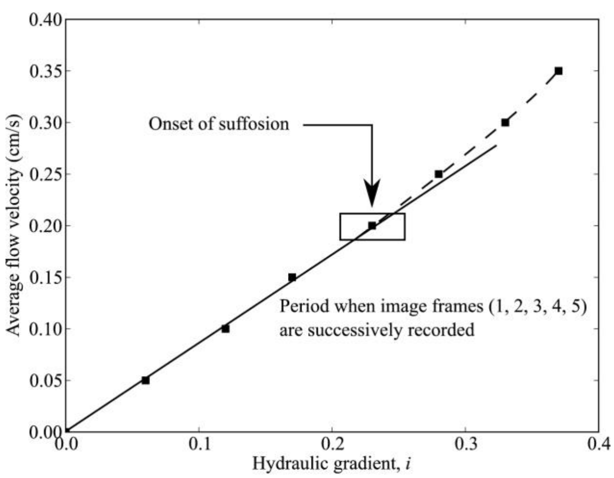

Fig. 6. Relationship between hydraulic gradient and average flow velocity (15% initial fines content)

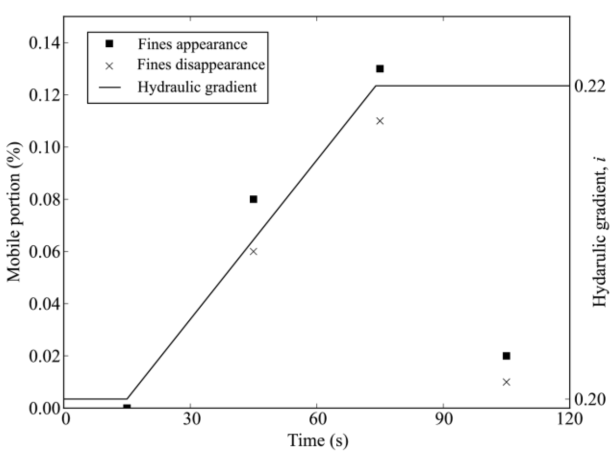

Fig. 7. Mobile portion during the onset of suffosion, together with the hydraulic gradient

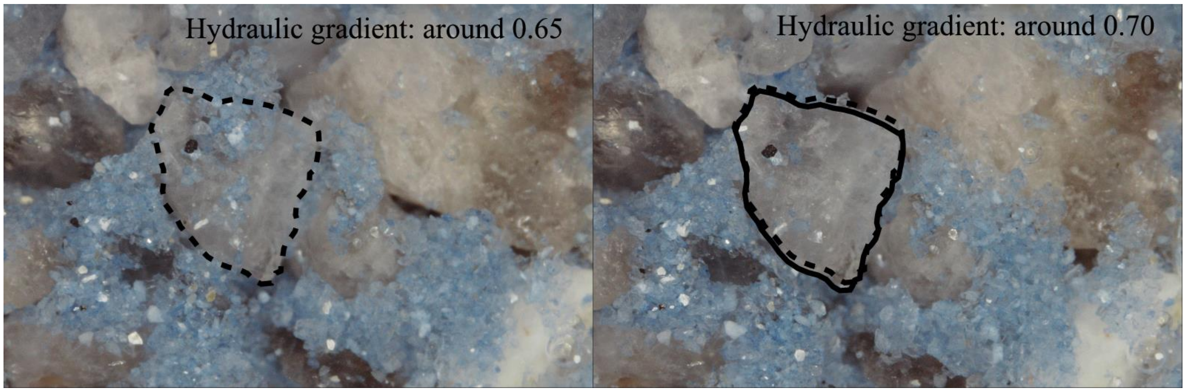

Fig. 8. Two selected images taken at hydraulic gradients equal to around 0.65 and 0.70 of specimen with 15% initial fines content: the dash line represents the outline of coarse particle at hydraulic gradient equals to around 0.65, while the solid line represents that at around 0.70

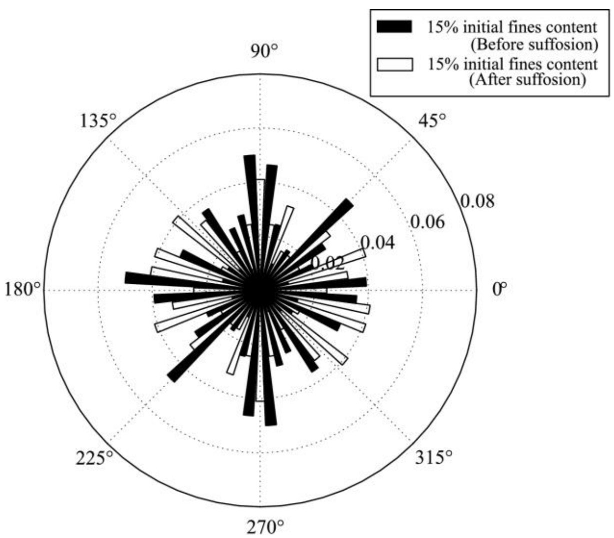

Fig. 9. Rose diagram representation of preferred coarse particles orientation of soil before and after suffosion